k-dependent optics of nanostructures: Spatial dispersion of metallic nanorings and split-ring resonators

Bruno Gompf,* Barbara Krausz, Bettina Frank, and Martin Dressel
Physikalisches Institut and Research Center SCOPE, Universität Stuttgart, Pfaffenwaldring 57, 70550 Stuttgart, Germany
(Received 27 September 2011; revised manuscript received 27 June 2012; published 27 August 2012)

The response of matter on an electromagnetic wave at a certain point and time depends on the field strength prior to this time and at places close to this point. Hence the material parameters are functions of the frequency ω and the wave vector $\vec{k}$, in general. While the temporal dispersion is common knowledge, spatial dispersion in usually disregarded. However it becomes crucial in the optical response of nanostructures. Here we map the complete $\vec{k}$-dependent optical response of a split-ring-resonator array over a broad frequency range via Mueller-matrix spectroscopic ellipsometry at different angles of incidence and all azimuthal orientations. The comparison with a closed-ring structure elucidates the rule of spatial dispersion in metal-dielectric nanostructures.

DOI: 10.1103/PhysRevB.86.075462 PACS number(s): 78.67.−n, 42.79.−e, 71.45.Gm, 73.20.Mf

I. INTRODUCTION

Maxwell's equations in the presence of matter are incomplete in the sense that they have to be amended by constitutive relations of $\vec{D}$ and $\vec{B}$ to $\vec{E}$ and $\vec{H}$. When choosing the common relations

$$\mathbf{D} = \underline{\epsilon}\mathbf{E} \quad \text{and} \quad \mathbf{B} = \underline{\mu}\mathbf{H}, \tag{1}$$

both material parameters, the dielectric permittivity $\underline{\epsilon}$ and the magnetic permeability $\underline{\mu}$, are second-rank tensors with components assumed to be a function of frequency in order to describe the time-dependent response. For a more general description one has to consider that an electric field can also lead to a magnetization and a magnetic field to a polarization. Including these effects, and looking only at the linear, local, and quasistatic response, the so-called bi-anisotropic constitutive relations exhibit the most general description:[1]

$$\vec{D} = \underline{\varepsilon}\vec{E} + \underline{\xi}\vec{H} \quad \text{and} \quad \vec{B} = \underline{\mu}\vec{H} + \underline{\zeta}\vec{E}. \tag{2}$$

Neglecting symmetry considerations, one ends up with 36 complex material parameters, which all depend on frequency but—and this is most important for the following—not on the wave vector $\vec{k}$. Although challenging, in principle they can be calculated *ab initio* from the atomic structure. The best test for band-structure calculations, for example, is still the comparison of theoretically obtained $\varepsilon(\omega)$ with the one determined by spectroscopy.[2] It has to be mentioned that from simple transmission or reflection measurements it is not possible to determine complex values, but generalized ellipsometry yields the information required for that comparison even for a triclinic crystal.[3] The coupling parameters ξ and ζ describe the magnetoelectric effects. Albeit known for more than hundred years, they have experienced a revival over the last 15 years.[4] One has to stress that all experiments for retrieving magnetoelectric coefficients were done in the kHz or MHz range where the quasistatic (long wavelength) limit is clearly fulfilled; i.e., Eq. (2) is unrestrictedly valid.

Approaches explicitly including nonlocal effects (spatial dispersion) were developed for the visible and near-infrared region, where the typical size of the building blocks of matter cannot be neglected compared to the wavelength of light anymore. In this spectral range no distinction can be made between the magnetic induction $\vec{B}$ and the magnetic field intensity $\vec{H}$ because $\mu = 1$ at optical frequencies.[5] Under this assumption the constitutive relations become rather simple:

$$\vec{D} = \varepsilon_{ij}(\omega,\vec{k})\vec{E} \quad \text{and} \quad \vec{B} = \vec{H}. \tag{3}$$

The elements of the dielectric tensor $\varepsilon_{ij}(\omega,\vec{k})$ in Eq. (3) can be expanded as a function of the wave vector $\vec{k}$:[6]

$$\varepsilon_{ij}(\omega,\vec{k}) = \varepsilon_{ij}(\omega) + \mathrm{i}\gamma_{ijm}(\omega)k_m + \alpha_{ijmn}(\omega)k_m k_n + \cdots. \tag{4}$$

As long as only the term linear in $\vec{k}$ is considered, bi-anisotropy [Eq. (2)] and spatial dispersion [Eq. (3)] represent equivalent descriptions;[7] i.e., the $\vec{k}$ dependence can be mimicked by a complex anisotropy.

II. OUTLINE OF THE PROBLEM

In crystal optics the regular building blocks of the material (atoms forming unit cells of size P) are small compared to the wavelength of light, $P \ll \lambda$; therefore spatial dispersion leads only to very small corrections in $\epsilon(\omega)$. In particular in highly symmetric crystals such as Si and GaAs the situation is very illustrative, because in crystals with inversion symmetry the terms linear in k in Eq. (4) vanish ($\gamma_{ijm} = 0$). Commonly they are treated as isotropic, but even for their small periodicities below one nanometer the k^2 term leads to a small but measurable anisotropy;[8,9] they exhibit a birefringence on the order of $\Delta n \approx 10^{-6}$ in their optical response. As mentioned above bi-anisotropy and spatial dispersion are only equivalent as long as higher order terms are neglected. Even for the description of the entire optical response of these simple semiconductors the $\vec{k}$ dependence has to be stated explicitly; it cannot be mapped on a bi-anisotropic behavior. The tensors γ_{ijm} and α_{ijmn} in Eq. (4) are of rank three and four, respectively; to the best of our knowledge they have not been defined experimentally or theoretically for crystals with lower symmetry.

For most nanostructures—dubbed metamaterials—the building blocks are in the range $\lambda/10 \leqslant P \leqslant \lambda/2$. To describe their optical behavior with effective optical parameters, a well-defined homogenization procedure has to be applied.[10,11] Classical effective medium approximations, such as Bruggeman's theory, are only valid in the long-wavelength limit.

These models fail in the description of disordered composites at higher filling factors[12] and they yield physically unreasonable effective optical parameters; for instance, they usually provide effective permittivities that are not Kramers-Kronig consistent.[13] The same is true for most retrieval procedures for effective permittivities and permeabilities from reflection and transmission measurements at normal incidence.[14] During the last couple of years it has become clear that in general it is not possible for these kinds of materials to define effective optical parameters, which are independent of the angle of incidence of the probing light.[15–18] In this context it is surprising that even for the model structure of metamaterials, the split-ring resonator, the complete $\vec{k}$-dependent optical response has not been measured up to now.

III. EXPERIMENTAL DETAILS

In this paper we present the optical properties of a large split-ring-resonator (SRR) array measured over the entire $\vec{k}$ space by Mueller-matrix spectroscopic ellipsometry[20] and compare the results with an array of closed rings (CRs) of the same size. The samples are prepared by shadow nanosphere lithography.[21] A densely packed hexagonal monolayer of 470 nm polystyrene spheres on a glass substrate is used as a mask, through which about 20 nm gold is evaporated. The samples are tilted by 17° with respect to normal and rotated about this axis during evaporation. A complete revolution produces closed rings with an inner diameter of about 50 nm and an outer diameter of 100 nm. Split-ring structures are obtained when the rotation is stopped before the circle is completed. By varying the opening angle, the resonance frequency of the SRR can be tuned.[22] This method enables us to produce a large area (10×10 mm^2) of periodic split-ring resonators as displayed in Fig. 1.

We characterized these structures by Mueller-matrix (MM) spectroscopic ellipsometry at various angles of incidence θ and azimuthal orientations α in the energy range of 0.5 to 3.5 eV (corresponding wavelength 2.5 to 0.35 μm). The measurements were performed in transmission utilizing a Woollam VASE spectroscopic ellipsometer, a polarizer-compensator-sample-rotating analyzer type instrument, which can determine 12 out of the 16 MM elements. It turns out that depolarization is negligible for our samples, and thus the number of relevant MM elements shrinks to ten. Hence the present incompleteness of the Mueller matrix by the missing fourth row does not constitute real limitations.

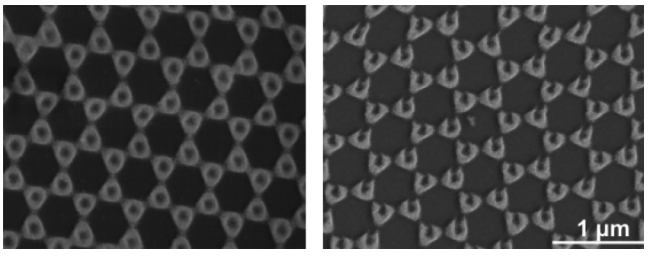

FIG. 1. Scanning electron micrograph of the investigated closed-ring structures (left) and the split-ring-resonator array (right).

IV. RESULTS

In Fig. 2 the transmission spectra at normal incidence are displayed for the two different samples of Fig. 1. The curves correspond to linear polarization parallel and perpendicular to the gap as indicated in the inset. For the CR structures only one well-pronounced resonance appears at about 0.8 eV. The slight shift between the two polarization states is due to minor deviations from the perfect circle that lift the degeneracy. In the case of split rings, the symmetry is completely broken. Correspondingly the SRR array gives a strongly anisotropic optical response: The resonances are shifted in opposite frequency directions for polarizations parallel and perpendicular to the gap. All observed resonances are predominantly plasmonic modes of the entire SRR or CR structure. By increasing the frequency, higher-order plasmonic modes are excited, which can be labeled according to the number of nodes in their out-of-plane electric-field component.[23] Light polarized parallel to the gap couples to modes in the SRR structure with an odd number of nodes, whereas modes with an even number of nodes are excited for perpendicular polarization. Upon closing the gap all odd modes vanish. The fact that higher-order modes can be excited at all is a consequence of the lateral extension of the structure. The size of the nanostructures is not negligible compared to the wavelength anymore. This gives a first hint that spatial dispersion can be important for these structures. As was pointed out by Rockstuhl *et al.*,[23] there is particularly no need to employ lump circuits, such as LC resonators.

From a simple transmission measurement at normal incidence it is not possible to judge whether a sample exhibits a purely dielectric response, which can be modeled by an $\underline{\varepsilon}$ tensor, or whether a more general model as described above

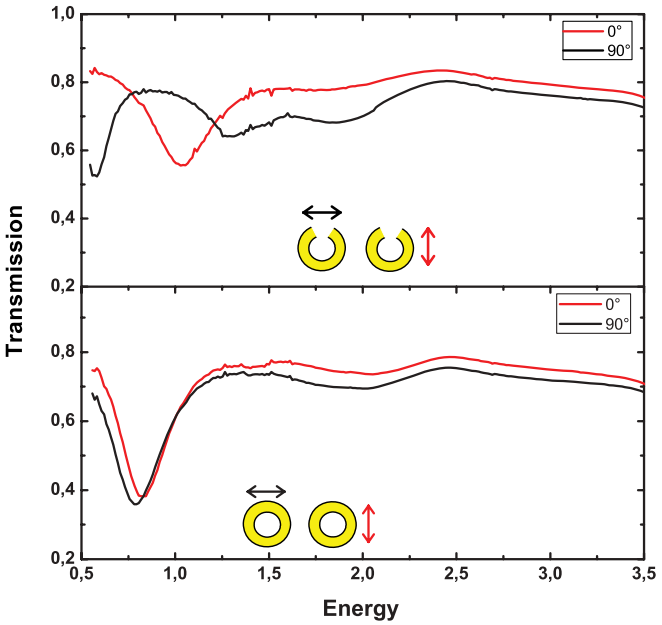

FIG. 2. (Color online) Transmission spectra at normal incidence of the split-ring-resonator (SRR) and closed-ring (CR) arrays. Whereas the CR appears nearly isotropic with a slight shift in the resonances between perpendicular directions, the SRR exhibits a strong dichroism.

is necessary to represent the entire optical behavior. To reveal anisotropy measurements at various azimuth orientations are necessary and spatial dispersion emerges only when the angle of incidence is varied. For a single angle of incidence, for example, the measured ellipsometric angles ψ and Δ of our samples can easily be modeled by a biaxial layer with two and three Lorentz oscillators perpendicular and parallel to the gap and one normal to the surface, respectively. With a similar model the optical response of simple gold disks of comparable size was recently described quite well.[24] At normal incidence this simple description provides also the transmission spectra displayed in Fig. 2. The problem is that in the case of the CR structure, one needs different parameters for each angle of incidence. Being interested in the complete optical response of the structure, we measured the MM elements $m_{ij}(\theta,\alpha,\omega)$ over the entire $\vec{k}$ space by varying the angle of incidence θ from 0° to 50° in steps of 4° and the azimuthal orientation α between 0° and 360° in 10° steps in the energy range between 0.5 and 3.5 eV. Mapping the complete ω and $\vec{k}$ dependencies accumulates a large amount of data. For reasons of clarity we restrict ourselves to the resonance energies at 0.8 eV for the CR array and 0.6 eV and 1.0 eV for the SRR array; here the MM elements reach their highest values; i.e., the mixing of polarization states is most pronounced. Outside the resonances the off-diagonal elements rapidly decay to zero.

To visualize the complex optical behavior of our nanostructures, we plot the MM elements in polar coordinates, where the radial component is the projection of the incident photon wave vector onto the plane of the sample: $|\vec{k}|\sin\theta$. The polar component corresponds to the azimuthal angle α. These plots map the complete $\vec{k}$ space at a given wavelength. The m_{ij} values are normalized to m_{11} and represented by a color code as indicated. This representation of the MM allows a very compact visualization of the entire optical response of anisotropic media. It has some similarities to conoscopic images known from crystal optics. One disadvantage is that the direct comparison to transmission measurements is not obvious. But from our measured MM elements the spectra shown in Fig. 2 can of course be obtained.[20]

For a first impression and for comparison in Fig. 3(b) a simulated MM contour plot for a 20 nm thick closed Au film on glass is shown. As expected for an isotropic sample, the upper right and the lower left (2×2) submatrices are zero[20] because the polarizations do not mix; i.e., incoming p-polarized light remains p polarized, and s-polarized light stays s polarized. We additionally measure the MM of a closed 20 nm thick Au film on glass. The agreement between experiment and simulation is nearly perfect. The experimental values for the upper right and the lower left (2×2) submatrices are below 10^{-3} in perfect agreement with the simulation. At a first glance for the hexagonal CR array one would expect a similar optical response. However the MM contour plot displayed in Fig. 3(a) is significantly more complex. Although the hexagonal CR structure is isotropic,[25] with increasing $|\vec{k}|$ the elements $m_{13}=m_{31}$ reveal small but measurable values giving unambiguous evidence that the polarization states mix at oblique incidence. For structures with inversion symmetry, like our hexagonal array, the third rank tensor γ_{ijk} in Eq. (4) indeed vanishes. Hence the polarization mixing of the CR

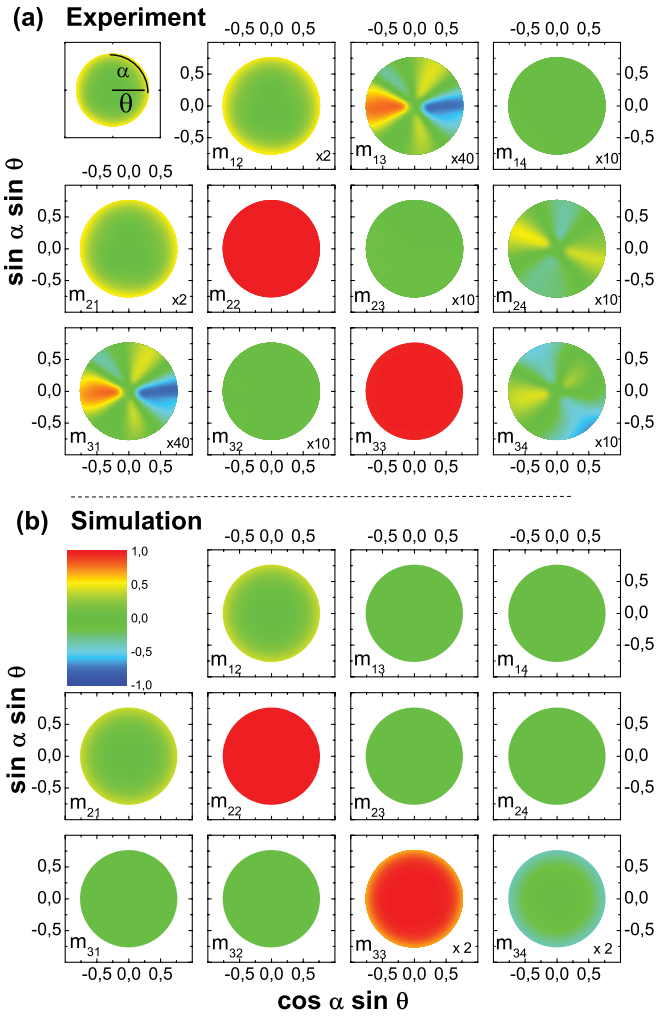

FIG. 3. (Color) (a) MM contour plot for the closed-ring array measured at 0.8 eV in transmission. In spite the isotropic lattice, the off-diagonal elements $m_{13}=m_{31}\neq 0$ clearly indicate a mixing of polarization states at oblique incidence. Note that some matrix elements are enhanced by a factor as indicated; m_{13} and m_{31} are multiplied by a factor of 40, for instance. (b) Simulated MM contour plot in transmission for a 20 nm closed Au film on glass. The upper right and the lower left (2×2) submatrices are zero; isotropic samples normally do not mix the polarization states at all.

array at oblique incidence is due to the k^2 term. The absolute values of m_{13} become as large as 0.02. This is huge when compared to the tiny birefringence of Si and GaAs, mentioned above. The building blocks of our CR array are orders of magnitude larger than that of the semiconductors, leading to Δn values comparable to quartz. Note that in classical optics, isotropic media mix the polarizations states of incoming light only when they are optically active. In the case of our CR structures this behavior is mimicked by spatial dispersion,[18] calling for a $\vec{k}$ optics. The optical response of the hexagonal CR structure is even more complex than that of the square hole array discussed in this paper.[18] Whereas, for example, the $m_{13}=m_{31}$ pattern of the square hole array exhibits inversion symmetry, the CR structure violates inversion symmetry. This does not mean that the samples are nonreciprocal, but they exhibit a optical response that is normally only known from

crystals or structures with very low symmetry, like slated nanocolumns, whose optical behavior can be described by monoclinic optical constants.[19] But opposite to crystals with symmetry lower than orthorhombic (skew unit cell), the MM patterns of the CR structure show no dispersion of the optic axes; i.e., the MM pattern does not rotate with energy. All these are strong hints that the optical response is dominated by the k^2 term in Eq. (4).

Before we discuss the MM contour plots of the SRR array, let us consider the Mueller matrix $\mathbf{M}$ in more detail. For a non-depolarizing, purely dielectric specimen, i.e., a sample where in Eq. (2) $\underline{\mu} = 1$ (nonmagnetic) and $\underline{\xi}$ and $\underline{\zeta}$ are zero (not optical active, reciprocal), the complete optical response is given by a Mueller matrix $\mathbf{M}$, which can be decomposed as[26]

$$\mathbf{M} = \mathbf{M_D}\mathbf{M_R}, \tag{5}$$

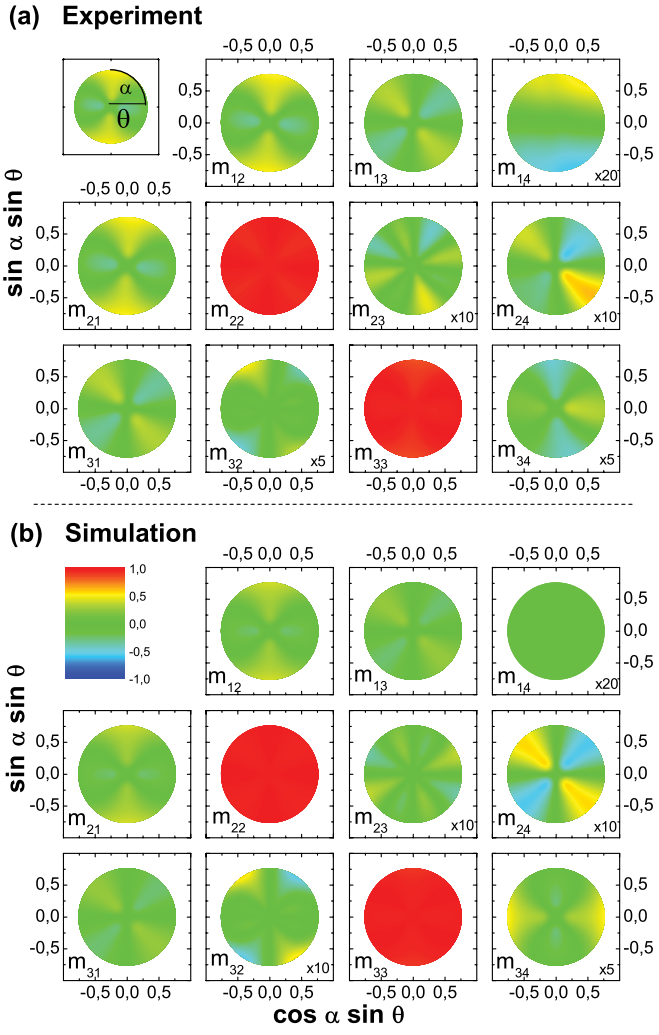

FIG. 4. (Color) (a) Measured and (b) simulated MM contour plots for the split-ring-resonator array at a given photon energy of 0.6 eV. For the simulations a simple in-plane anisotropy was used with two and three Lorentz oscillators in the two perpendicular directions, respectively. This model describes the overall optical response of the SRR array very well. It is not necessary to assume any permeability $\mu \neq 1$.

where the diattenuator matrix $\mathbf{M_D}$ acts on the intensity only (i.e., ideal polarizer), and the retarder matrix $\mathbf{M_R}$ changes the phase depending on the incident polarization (i.e., ideal retarder). For dielectric samples with an in-plane anisotropy, the MM element m_{13} exhibits a $\sin\{2\alpha\}$ dependence and the element m_{23} has a $\cos\{2\alpha\}\sin\{2\alpha\}$ dependence on the azimuth orientation α.[20] Note that for all MMs which can be decomposed as in Eq. (5), the first row and the first column are transposed to each other. Depolarization effects lift this correlation. The fact that all our measured MMs exhibits the property $m_{1i} = m_{i1}$ provides clear evidence that depolarization effects can be neglected in our investigations.

In Fig. 4 the measured MM contour plots of our SRR array are displayed together with the simulated ones obtained from the anisotropic model that has been utilized above to explain the transmission (Fig. 2). It has to be mentioned that going from the resonance at 0.6 eV to the one at 1.0 eV simply rotates the MM pattern of the off-diagonal elements by 90°. The SRR array exhibits an optical response, which can be perfectly described by a biaxial layer of 20 nm thickness with two Lorentz oscillators for the direction perpendicular and three oscillators for the direction parallel to the gap and one oscillator normal to the surface. In contrast to the CR array, for instance, for the SRR array the azimuthal dependence of the element m_{13} nicely follows the behavior expected for a purely dielectric sample with a strong in-plane dichroism ($m_{13} \propto \sin\{2\alpha\}$). In particular, there is no need to introduce any kind of permeability to model the entire optical response of SRR arrays.

It should be noted that spatial dispersion is also present in the SRR sample, however, much weaker than the dichroism in the resonance of the SRRs, and therefore it does not appear in Fig. 4. In the case of the CR structure presented in Fig. 3, the MM element m_{13}, for example, is magnified by a factor of 40.

V. DISCUSSION AND CONCLUSION

Going back to our original question of how to describe the electrodynamic properties of nanostructures, we have to conclude that bi-anisotropic constitutive relations [Eqs. (2)] cannot explain the entire optical response of our test samples. The Mueller-matrix contour plots especially reveal the role of spatial dispersion in the optical behavior of artificial nanostructures. With the expansion given in Eq. (4), the $\vec{k}$-dependent behavior can in principle be well described, but one has to be aware that the tensors γ_{ijm} and α_{ijmn} are of rank three and four, respectively; i.e., a huge number of effective optical parameters are needed for their proper description. Keeping this in mind, the question arises as to whether the concept of effective optical parameters is applicable at all, or whether for the proper treatment of nanostructures the full three-dimensional boundary conditions have to be taken into account.

ACKNOWLEDGMENTS

We acknowledge discussions with H. Giessen and H. Schweizer. The work was supported by the Deutsche Forschungsgemeinschaft (GO642/7).

*gompf@pi1.physik.uni-stuttgart.de

[1] A. Serdyukov, I. Semchenko, S. Tretyakov, and A. Sihvola, *Electromagnetics of Bi-anisotropic Materials: Theory and Application* (Gordon and Breach Science Publishers, 2001).

[2] P. Y. Yu and M. Cardona, *Fundamentals of Semiconductors* (Springer, Berlin, 1996).

[3] M. Dressel, B. Gompf, D. Faltermeier, A. K. Tripathi, J. Pflaum, and M. Schubert, Opt. Express **16**, 19770 (2008).

[4] M. Fiebig, J. Phys. D **38**, R123 (2005).

[5] L. D. Landau and E. M. Lifshitz, *Electrodynamics of Continuous Media* (Pergamon Press, 1984).

[6] V. M. Agranovich and V. L. Ginzburg, *Crystal Optics with Spatial Dispersion and Excitons* (Springer, Berlin, 1984).

[7] R. M. Hornreich and S. Shtrikman, Phys. Rev. **171**, 1065 (1968).

[8] J. Pastrnak and K. Vedam, Phys. Rev. B **3**, 2567 (1971).

[9] P. Y. Yu and M. Cardona, Solid State Commun. **9**, 1421 (1971).

[10] I. Tsukerman, J. Opt. Soc. Am. B **23**, 577 (2011).

[11] C. R. Simovski, J. Opt. **13**, 013001 (2011).

[12] M. Hövel, B. Gompf, and M. Dressel, Phys. Rev. B **81**, 035402 (2010).

[13] T. C. Choy, *Effective Medium Theory* (Clarendon Press, Oxford, 1999).

[14] D. R. Smith, S. Schultz, P. Markos, and C. M. Soukoulis, Phys. Rev. B **65**, 195104 (2002).

[15] C. Menzel, C. Rockstuhl, T. Paul, F. Lederer, and T. Pertsch, Phys. Rev. B **77**, 195328 (2008).

[16] C. Menzel, C. Helgert, J. Üpping, C. Rockstuhl, E.-B. Kley, R. B. Wehrspohn, T. Pertsch, and F. Lederer, Appl. Phys. Lett. **95**, 131104 (2009).

[17] C. Menzel, T. Paul, C. Rockstuhl, T. Pertsch, S. Tretyakov, and F. Lederer, Phys. Rev. B **81**, 035320 (2010).

[18] B. Gompf, J. Braun, T. Weiss, H. Giessen, M. Dressel, and U. Hübner, Phys. Rev. Lett. **106**, 185501 (2011).

[19] D. Schmidt, B. Booso, T. Hofmann, E. Schubert, A. Saragan, and M. Schubert, Appl. Phys. Lett. **94**, 011914 (2009).

[20] D. Goldstein, *Polarized Light* (Marcel Dekker Inc., New York, 2003).

[21] A. Kosiorek, W. Kandulski, P. Chudzinski, K. Kempa, and M. Giersig, Nano Lett. **4**, 1359 (2004).

[22] M. C. Gwinner, E. Koroknay, L. Fu, P. Patoka, W. Kundulski, M. Giersig, and H. Giessen, small **5**, 400 (2009).

[23] C. Rockstuhl, F. Lederer, C. Etrich, T. Zentgraf, J. Kuhl, and H. Giessen, Opt. Express **14**, 8827 (2006).

[24] A. Mendoza-Galvan, K. Järrendahl, A. Dmitriev, T. Pakizeh, M. Käll, and A. Arwin, Opt. Express **19**, 12093 (2011).

[25] C. Menzel, C. Rockstuhl, and F. Lederer, Phys. Rev. A **82**, 053811 (2010).

[26] Shih-Yau Lu and R. A. Chipman, J. Opt. Soc. Am. A **13**, 1106 (1996).